

Driven k -mers: Correlations in space and time

Shamik Gupta,^{1,2,3} Mustansir Barma,¹ Urna Basu,⁴ and P. K. Mohanty⁴

¹*Department of Theoretical Physics, Tata Institute of Fundamental Research, Homi Bhabha Road, Mumbai 400005, India*

²*Physics of Complex Systems, Weizmann Institute of Science, Rehovot 76100, Israel*

³*Laboratoire de Physique de l'École Normale Supérieure de Lyon, Université de Lyon, CNRS, 46 Allée d'Italie, 69364 Lyon cédex 07, France*

⁴*Theoretical Condensed Matter Physics Division, Saha Institute of Nuclear Physics, Kolkata 700064, India*

(Dated: November 12, 2018)

Steady-state properties of hard objects with exclusion interaction and a driven motion along a one-dimensional periodic lattice are investigated. The process is a generalization of the asymmetric simple exclusion process (ASEP) to particles of length k , and is called the k -ASEP. Here, we analyze both static and dynamic properties of the k -ASEP. Density correlations are found to display interesting features, such as pronounced oscillations in both space and time, as a consequence of the extended length of the particles. At long times, the density autocorrelation decays exponentially in time, except at a special k -dependent density when it decays as a power law. In the limit of large k at a finite density of occupied sites, the appropriately scaled system reduces to a nonequilibrium generalization of the Tonks gas describing the motion of hard rods along a continuous line. This allows us to obtain in a simple way the known two-particle distribution for the Tonks gas. For large but finite k , we also obtain the leading-order correction to the Tonks result.

PACS numbers: 05.70.Ln, 05.60.Cd, 87.10.Hk

I. INTRODUCTION

The asymmetric simple exclusion process (ASEP), a paradigmatic model of nonequilibrium statistical mechanics, involves hard-core particles undergoing biased diffusion on a lattice in the presence of an external drive [1–5]. The generalization of the ASEP to an exclusion process of hard-core extended objects (k -mers, each of which occupies k consecutive sites) is referred to as the k -ASEP. It was first introduced to model protein synthesis inside living cells [6, 7]. During the synthesis, ribosomes move from codon to codon along messenger RNA, read off genetic information, and generate the protein stepwise. Modelling the codons by lattice sites and the ribosomes by k -mers, we recover the k -ASEP. The spatial extent of the k -mers takes care of the blocking of several codons by a single ribosome; steric hindrance, which prevents overlap of ribosomes, is modelled by the exclusion constraint.

Earlier studies of the k -ASEP in one dimension involved analyzing the steady-state density profile in an open system [6, 7], the time-dependent conditional probabilities of finding the k -mers on specific sites at a given time [8], the dynamical exponent [9], the phase diagram of the system with open boundaries [10–13], the hydrodynamic limit governing the evolution of the density [14], and the effects of defect locations on the lattice on steady-state properties [15, 16]. Some aspects of the $k = 2$ case of the k -ASEP were studied earlier in the context of a model of driven, reconstituting dimers [17].

Here, we are concerned with the k -ASEP on a one-dimensional (1D) periodic lattice. At long times, the process settles into a nonequilibrium steady state in which all configurations with a given number of k -mers have

equal weights [11]. In this work, our focus is on correlation functions, both static and dynamic.

We compute static correlations in two different ways: (i) by counting the number of relevant configurations, and (ii) by mapping the k -ASEP to a zero-range process (ZRP) [18] and then by employing a matrix product formalism [19]. Dynamic correlations in the k -ASEP are derived by mapping the k -ASEP to an equivalent ASEP with a smaller number of sites and by using the known dynamic properties of the latter [17]. We show that density correlations exhibit pronounced oscillations in both space and time as a consequence of the extended length of the k -mers.

One may also consider the k -ASEP in the continuum limit, i.e., in the joint limit of large k and vanishing lattice spacing, $\delta \rightarrow 0$, while keeping the product $a = k\delta$ and the density of occupied sites fixed and finite. Such a limit was considered previously to obtain the hydrodynamic behavior of the continuum system [20]. In this limit, the model describes hard rods of finite length a , undergoing biased diffusion along a continuous line in the presence of an external drive. In the case of unbiased motion, this continuum model was studied earlier by Tonks [21]. This so-called Tonks gas has an equilibrium steady state in which quantities of physical interest, e.g., the equation of state and the two-particle distribution function, have been worked out exactly [21, 22]. The continuum limit of the k -ASEP is a nonequilibrium generalization, and may be called the driven Tonks gas.

The known two-particle distribution function of the Tonks gas is recovered straightforwardly by taking the continuum limit of the k -ASEP, on noting that the steady-state measure of configurations is the same, whether or not the system is driven. We also obtain the leading-order correction to the Tonks result when k

is large but finite. The Tonks result, after including the leading-order correction in $1/k$, turns out to be a good approximation to the k -ASEP equal-time spatial correlation even for not too large values of k (for example, $k = 13$ when the density of occupied sites is 0.75).

The paper is organized as follows. In Sec. II, we define the k -ASEP and discuss its steady-state measure. In the following section, we derive closed-form expressions for the steady-state equal-time engine-engine and density-density correlations. The former function describes correlation between the right end (the “engine”) of one k -mer with that of another at the same time instant. Considering the continuum limit of the k -ASEP, we derive the known two-particle distribution function for the Tonks gas. We also derive the leading finite- k correction to the Tonks result. In Sec. IV, we address the steady-state dynamics by computing the k -mer current and kinematic wave velocity associated with transport of density fluctuations. We then discuss a mapping of the k -ASEP to an equivalent ASEP, and the behavior of the k -ASEP temporal density-density correlation, whose scaling properties are derived by utilizing the mapping. In Appendix A, we discuss a different method to obtain static correlations in the k -ASEP through a mapping to an equivalent ZRP.

II. THE k -ASEP

A. Definition

We consider a number, N , of k -mers that are subject to hard-core exclusion and are distributed on a 1D periodic lattice of L sites. The sites are labeled by the index $i = 1, 2, \dots, L$. Each k -mer occupies k consecutive lattice sites. The k -mers are hard objects that cannot break into smaller fragments. The density of occupied sites in the system is given by

$$\rho \equiv \frac{Nk}{L}. \quad (1)$$

We specify the location of a k -mer on the lattice by the site index of its rightmost end, and we call this end the “engine” of the k -mer. We denote the occupation of the i th site by $n_i = 1$ or 0, according to whether the site is occupied or vacant, respectively. A k -mer is then represented by a string of k consecutive 1’s and a configuration of the model by an L -bit binary string composed of 0’s and 1’s.

The system of k -mers evolves according to a stochastic Markovian dynamics: in a small time dt , a k -mer advances forward (respectively, backward) by one lattice site with probability pdt (respectively, qdt), provided the site is unoccupied. The dynamics conserves the total number of k -mers in the system. The elementary dynamical moves may be represented as

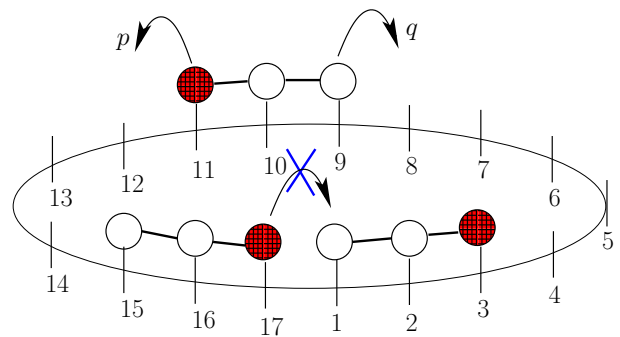
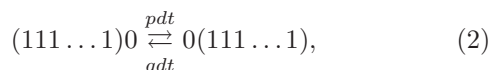


FIG. 1: (Color online) The k -ASEP on a ring, showing the allowed and disallowed dynamical moves of trimers ($k = 3$). Here, k -mers are represented as k connected circles. The rightmost end of a k -mer (the “engine”) is indicated by a filled red circle.

where the k -mer has been represented by a string of k consecutive 1’s enclosed by brackets. Figure 1 illustrates the allowed and disallowed moves of trimers ($k = 3$).

For $p \neq q$, the k -mers move preferentially in one direction along the lattice, and the system at long times reaches a nonequilibrium steady state with a steady current of k -mers.

When $p = q$, the k -mers diffuse symmetrically to the left and to the right. In this case, the model is a generalization of the symmetric simple exclusion process (SEP) of hard-core particles to k -mers, and may be referred to as the k -SEP. At long times, the k -SEP settles into an equilibrium steady state.

B. Relation to a model of diffusing, reconstituting dimers

Earlier studies of a variant of the k -ASEP dealt with dimers ($k = 2$) that, in general, do not retain their identities and are allowed to reconstitute [17, 23]. Specifically, on a lattice of L sites, single particles or monomers (denoted by 1) and paired particles or dimers (denoted by 11) are distributed with at most one particle per site. The dynamics in a small time dt involves a dimer moving by one lattice site, either forward with probability pdt or backward with probability qdt , without violating the hard-core constraint on site occupancies. The pairing of the dimers is impermanent, thereby allowing for reconstitution. For example, in the sequence of transitions, $11010 \rightarrow 01110 \rightarrow 01011$, the middle particle is paired with the particle to the left in the first transition and with the particle to the right in the second transition.

Both in the symmetric ($p = q$) [23] and in the asymmetric ($p \neq q$) [17] case, the phase space of the system breaks up into an infinite number of dynamically disjoint sectors. A non-local construct, called the irreducible string (IS), uniquely labels the different sectors. The IS for a given configuration is constructed from

the corresponding L -bit binary string by deleting recursively any pair of adjacent 1's until no further deletion is possible. The model exhibits dynamical diversity with quantities like the density autocorrelation showing strong sector-dependent behaviors that range from power laws to stretched exponentials.

The problem of hard non-reconstituting dimers, i.e. the case $k = 2$ of the k -mer system considered in this work, corresponds to a particular sector of the reconstituting dimer problem, namely, the one with the null IS 0000...000. It is easy to check that this is the sector in which dimers do not reconstitute.

C. The steady state

In the steady state of the k -ASEP, every microscopic configuration C with a given number of k -mers is equally likely, and hence, occurs with probability $1/\Omega$, where Ω is the total number of configurations [11]. In such a state, for every transition away from C to another configuration C' , it is simple to construct a distinct and unique configuration C'' that evolves to C at the same rate, thereby ensuring stationarity. This argument holds for periodic boundary conditions and fails in the case of open boundaries where the exact steady state is hard to obtain and is as yet unknown.

Now, Ω is determined by counting the different possible ways of distributing a number, N , of k -mers over a lattice of L sites with periodic boundaries. First consider *free* boundaries, in which case we have an open chain of L sites on which the k -mers are placed. Then, the number of possible ways of distributing the k -mers is

$$\Omega_{N,L}^{\text{free}} = \binom{L - Nk + N}{N}. \quad (3)$$

For a periodic lattice, the number of ways is determined by first considering all configurations in which an arbitrary but fixed site remains occupied by an arbitrarily chosen but fixed engine. The number of such configurations is simply $\Omega_{N-1,L-k}^{\text{free}}$. However, the engine could be chosen to be one of the N identical engines available and may be placed over any of the available L sites. Thus, the total number of distinct configurations is [11]

$$\Omega = \frac{L}{N} \Omega_{N-1,L-k}^{\text{free}} = \frac{L}{N} \binom{L - Nk + N - 1}{N - 1}. \quad (4)$$

The steady-state probability that a randomly chosen site is occupied by an engine is obtained by considering all possible ways of distributing a number, $N - 1$, of k -mers over a lattice of $L - k$ sites with free boundaries. Since all configurations of the k -ASEP are equally likely in the steady state, the desired probability is given by the ratio $\Omega_{N-1,L-k}^{\text{free}}/\Omega = \rho/k$. Similarly, the probability that a randomly chosen site is vacant in the steady state may be shown to be equal to $1 - \rho$. Next, we consider the joint probability that in the steady state, a randomly chosen

site is occupied by an engine while the following site is vacant; this is given by the ratio $\Omega_{N-1,L-(k+1)}^{\text{free}}/\Omega$. In the thermodynamic limit, i.e. in the limit $N \rightarrow \infty, L \rightarrow \infty$, while keeping k and ρ fixed and finite, this joint probability equals $\rho(1 - \rho)/[\rho + k(1 - \rho)]$.

We note that for the k -SEP, the condition of detailed balance implies that all configurations with a given number of k -mers have equal weights in its equilibrium steady state. It thus follows that the exclusion process with k -mers has the same steady state, irrespective of whether the k -mers have a biased or an unbiased motion.

III. STEADY STATE STATICS

A. Engine-engine correlation

Let E_i denote the engine occupation variable for site i , taking values 1 or 0 according to whether the site is occupied by an engine or not, respectively. The (unsubtracted) equal-time engine-engine correlation function $\mathcal{E}_k(r)$ is defined as

$$\mathcal{E}_k(r) \equiv \langle E_i E_{i+r} \rangle, \quad (5)$$

where the angular brackets denote averaging with respect to the steady state. Note that $\mathcal{E}_k(r)$ is identically zero for $r < k$.

Now, $\mathcal{E}_k(r)$ for $r \geq k$ has non-zero contributions from all configurations in which there are two engines at the i -th and $(i + r)$ -th sites, with the gap between the two engines containing $r - k$ sites that are occupied by any number, m , of k -mers between 0 and the maximum number that may be placed in the gap, while the left over $N - (m + 2)$ number of k -mers is distributed over the remaining $L - (r - k + 2k)$ sites. The maximum number of k -mers that may be placed over the gap of $r - k$ sites is given by $\lfloor (r - k)/k \rfloor$, where $\lfloor x \rfloor$ denotes the floor function that gives the largest integer not greater than x . Noting that in the steady state of the k -ASEP, all configurations have equal weights, we get

$$\mathcal{E}_k(r) = \sum_{m=0}^{\lfloor (r-k)/k \rfloor} \frac{\Omega_{m,r-k}^{\text{free}} \Omega_{N-m-2,L-r-k}^{\text{free}}}{\Omega}. \quad (6)$$

In the thermodynamic limit, one can show by using Eq. (3) that, for arbitrary integers m_1 and m_2 ,

$$\frac{\Omega_{N-m_1,L-m_2}^{\text{free}}}{\Omega_{N,L}^{\text{free}}} = \rho_0^{m_1} (1 - \rho_0)^{m_2 - m_1 k}, \quad (7)$$

where

$$\rho_0 \equiv \frac{\rho}{k(1 - \rho) + \rho}. \quad (8)$$

Later, in Sec. IV, by using a mapping of the k -ASEP to the usual ASEP, we show that the quantity ρ_0 is in fact

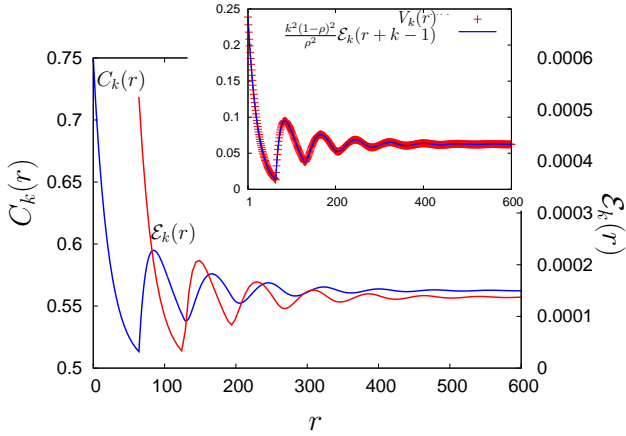


FIG. 2: (Color online) The k -ASEP density-density correlation $C_k(r)$ and engine-engine correlation $\mathcal{E}_k(r)$, evaluated numerically by using Eqs. (12) and (9) for $k = 64$ and $\rho = 0.75$. The inset shows that $V_k(r)$ and $[k^2(1-\rho)^2/\rho^2]\mathcal{E}_k(r+k-1)$ are equal, in agreement with Eq. (17).

the particle density in the latter. Using Eq. (7), we find that in the thermodynamic limit, Eq (6) reduces to

$$\mathcal{E}_k(r) = \frac{\rho_0^2}{1 + \rho_0(k-1)} \times \sum_{m=0}^{\lfloor (r-k)/k \rfloor} \binom{r-k-km+m}{m} \rho_0^m (1-\rho_0)^{r-k-km}; \quad r \geq k. \quad (9)$$

For $k = 2$, the sum in Eq. (9) can be evaluated exactly to obtain $\mathcal{E}_k(r) = \frac{\rho_0^2}{(1+\rho_0)^2} [1 - (-\rho_0)^{r-1}]$ [17]. For $k \geq 3$, the function $\mathcal{E}_k(r)$ may be numerically evaluated by using Eq. (9). Figure 2 shows the result for $k = 64$. We see that the engine-engine correlation exhibits damped oscillations in space, a hallmark of systems with hard-core interactions between the constituents [24], where purely entropic considerations apply. For example, the fact that $\mathcal{E}_k(r)$ has its first minimum at $r = 2k - 1$ and rises again at $r = 2k$ may be understood to be due to the possibility that when $r = 2k$, there may be configurations with an additional engine between the two engines that are occupying sites i and $i + 2k$.

B. Density-density correlation

The (unsubtracted) equal-time density-density correlation function $C_k(r)$ is defined as

$$C_k(r) \equiv \langle n_i n_{i+r} \rangle. \quad (10)$$

Here, n_i is the occupation variable for site i , taking values 1 or 0, according to whether the site is occupied or is vacant, respectively. Evidently, n_i can be expressed in

terms of the engine occupation variable E_i as

$$n_i = \sum_{m=0}^{k-1} E_{i+m}. \quad (11)$$

Using the above equation, $C_k(r)$ may be expressed in terms of the equal-time engine-engine correlation as

$$C_k(r) = k\mathcal{E}_k(r) + \sum_{m=1}^{k-1} m \left[\mathcal{E}_k(r+k-m) + \mathcal{E}_k(r-k+m) \right], \quad (12)$$

where it is understood that $\mathcal{E}_k(r)$ is zero for $r < k$.

Alternatively, $C_k(r)$ can be computed in a straightforward way from the equal-time vacancy-vacancy correlation, defined as

$$V_k(r) \equiv \langle \bar{n}_i \bar{n}_{i+r} \rangle, \quad (13)$$

where $\bar{n}_i = 1 - n_i$, so that

$$C_k(r) = V_k(r) + (2\rho - 1). \quad (14)$$

Now, $V_k(r)$ for $r \geq 1$ has non-zero contributions from all configurations in which both the i -th and $(i+r)$ -th sites are vacant, with the gap between the two containing $r-1$ sites that are occupied by any number, m , of k -mers between 0 and the maximum number that may be placed in the gap, while the left over $N-m$ number of k -mers is distributed over the remaining $L - (r-1+2)$ sites. We get

$$V_k(r) = \sum_{m=0}^{\lfloor (r-1)/k \rfloor} \frac{\Omega_{m,r-1}^{\text{free}} \Omega_{N-m,L-r-1}^{\text{free}}}{\Omega}. \quad (15)$$

In the thermodynamic limit, we find that

$$V_k(r) = \frac{(1-\rho_0)^2}{1+\rho_0(k-1)} \times \sum_{m=0}^{\lfloor (r-1)/k \rfloor} \binom{r-1-km+m}{m} \rho_0^m (1-\rho_0)^{r-1-km}; \quad r \geq 1. \quad (16)$$

It follows from the definition that $V_k(0) = 1 - \rho$. On comparing Eq. (16) with Eq. (9), and noting that $(1-\rho_0)^2/\rho_0^2 = k^2(1-\rho)^2/\rho^2$, we get

$$V_k(r) = \frac{k^2(1-\rho)^2}{\rho^2} \mathcal{E}_k(r+k-1); \quad r \geq 1. \quad (17)$$

Using Eq. (14), we get

$$C_k(r) = \frac{k^2(1-\rho)^2}{\rho^2} \mathcal{E}_k(r+k-1) + (2\rho - 1); \quad r \geq 1. \quad (18)$$

For $r = 0$, we have $C(0) = \rho$.

Figure 2 shows $C_k(r)$, computed using Eqs. (12) and (9), for $k = 64$ and $\rho = 0.75$. The oscillations in $C_k(r)$

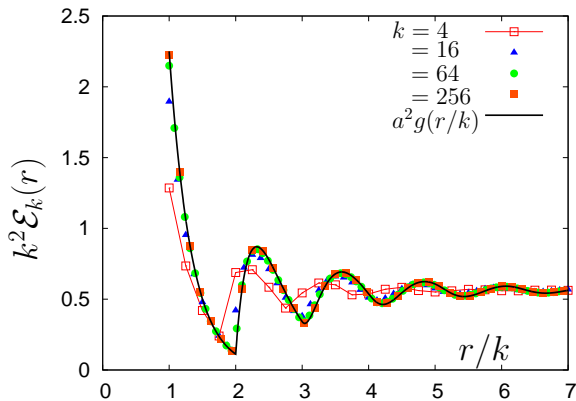


FIG. 3: (Color online) Scaling approach of the engine-engine correlation $\mathcal{E}_k(r)$ to the Tonks limit: $k^2 \mathcal{E}_k(r)$ vs. r/k at fixed $\rho = 0.75$ and $a = 400$ shows data collapse for large k according to Eq. (23).

may be related to those in $\mathcal{E}_k(r)$ by using Eq. (18). For instance, since $\mathcal{E}_k(r)$ has its first minimum at $r = 2k - 1$, it follows that the first minimum of $C_k(r)$ occurs at $r = k$. The inset of Fig. 2 shows that $V_k(r)$ and $[k^2(1 - \rho)^2/\rho^2]\mathcal{E}_k(r + k - 1)$ for $r \geq 1$ are equal in accordance with Eq. (17).

Later, in Appendix A, we discuss an alternative method to obtain static correlations in the k -ASEP through a mapping to a zero-range process and employing a matrix product formalism [19].

C. Continuum limit: Driven Tonks gas

In a suitable continuum limit of the k -ASEP, discussed below, the model reduces to one of hard rods, which have exclusion interaction, and which are undergoing driven, diffusive motion along a continuous line. In the absence of drive, this continuum model was studied by Tonks as a 1D interacting system with an equilibrium steady state in which thermodynamic properties like the equation of state can be worked out exactly [21]. When the motion is driven, the continuum limit of the k -ASEP becomes the driven Tonks gas.

A quantity of physical interest for the equilibrium Tonks gas is the two-particle distribution $P(R_1, R_2)$, defined such that $P(R_1, R_2)dR_1dR_2$ is the joint probability of finding the rightmost end of one hard rod between R_1 and $R_1 + dR_1$ and that of another between R_2 and $R_2 + dR_2$. For a translationally invariant system, $P(R_1, R_2)$ is a function of the separation $R \equiv |R_2 - R_1|$.

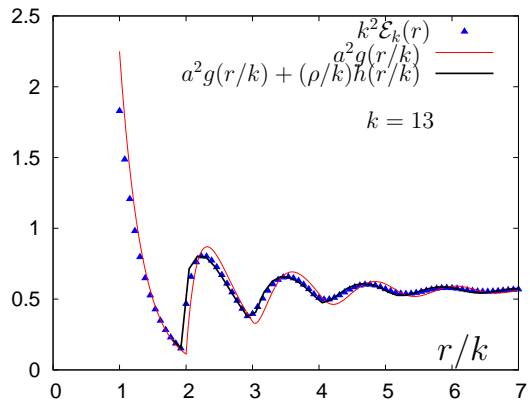


FIG. 4: (Color online) Comparison of $k^2 \mathcal{E}_k(r)$ with the Tonks result, $a^2 g(r/k)$, for $k = 13$, $a = 400$, and $\rho = 0.75$, showing the discrepancy between the two for large but finite k . The discrepancy is resolved on including the correction to the Tonks result, to leading order in $1/k$, as is shown by a comparison of $k^2 \mathcal{E}_k(r)$ with the function $a^2 g(r/k) + (\rho/k)h(r/k)$ (Eq. (25)).

Then, if a is the rod length, it is known that [22]

$$P(R) = g(x),$$

$$g(x) \equiv \frac{1}{la^2} \sum_{m=1}^{\infty} A(x-m) \frac{(x-m)^{m-1}}{(m-1)!(l-1)^m}$$

$$\times \exp\left(-\frac{x-m}{l-1}\right), \quad (19)$$

where $x = R/a$ is a reduced distance. Here, $l = 1/a\rho_T$, where ρ_T is the density of rods, and $A(x)$ is the unit step function:

$$A(x) = \begin{cases} 0 & \text{for } x < 0, \\ 1 & \text{for } x \geq 0. \end{cases} \quad (20)$$

We now show that the continuum limit of the k -ASEP engine-engine correlation easily yields Eq. (19). Such a derivation is justified by the fact that, as discussed in Sec. II C, the k -ASEP has the same steady-state measure of configurations for both unbiased and biased motion of the k -mers. This fact further implies that Eq. (19) also holds for the driven Tonks gas.

The continuum limit of the k -ASEP is obtained by considering the joint limit $k \rightarrow \infty$, $r \rightarrow \infty$, and the lattice spacing $\delta \rightarrow 0$, while keeping $R = r\delta$, $a = k\delta$, and ρ fixed and finite [20]. The k -ASEP then describes biased motion of hard rods of length a along a continuous line. The density of hard rods is $\rho_T = \rho/a$. In this limit, when $\rho_0 = \rho\delta/[a(1-\rho)]$ and $(1-\rho_0) = \exp[-\rho\delta/[a(1-\rho)]]$,

Eq. (9) reduces to

$$\mathcal{E}_k(r) = \frac{\delta^2}{l a^2} \sum_{m=0}^{\lfloor R/a-1 \rfloor} \frac{[R/a - (m+1)]^m}{m!(l-1)^{m+1}} \times \exp\left(-\frac{R/a - (m+1)}{l-1}\right). \quad (21)$$

Comparing the right-hand side of the last equation with Eq. (19), and noting that $R/a = r/k$, we find that

$$\mathcal{E}_k(r) = \delta^2 g\left(\frac{r}{k}\right). \quad (22)$$

Now, since $\delta = a/k$, we find that in the continuum limit, i.e., in the limit $k \rightarrow \infty$, $r \rightarrow \infty$, $\delta \rightarrow 0$, while keeping a , R , and ρ fixed and finite, $\mathcal{E}_k(r)$ for different k has the scaling form

$$\mathcal{E}_k(r) = \frac{a^2}{k^2} g\left(\frac{r}{k}\right). \quad (23)$$

Moreover, in the continuum limit, defining $P(R) = \mathcal{E}_k(r)/\delta^2$, we find from Eq. (22) that $P(R)$ is precisely in the form of Eq. (19). We have thus derived the two-particle distribution, valid for both the equilibrium and the driven Tonks gas, by considering the continuum limit of the k -ASEP.

Figure 3 shows plots of $k^2 \mathcal{E}_k(r)$ for different k at fixed ρ and a , evaluated using Eq. (9). As k increases, the curves show a good scaling collapse, in accordance with Eq. (23). For large but finite k , the right-hand side of Eq. (23) has finite- k corrections, as is suggested by the discrepancy between $k^2 \mathcal{E}_k(r)$ and $a^2 g(r/k)$, shown in Fig. 4. The leading-order correction to Eq. (23) will be discussed in the following subsection.

The behavior of the density correlation $C_k(r)$ in the continuum limit may be easily obtained by using Eqs. (18) and (23). We find that in this limit, for different k at fixed ρ and a , we have

$$C_k(r) = \frac{a^2(1-\rho)^2}{\rho^2} g\left(\frac{r}{k} + 1\right) + (2\rho - 1). \quad (24)$$

Figure 5 shows plots of $C_k(r)$ for different k at fixed ρ and a , evaluated using Eqs. (9) and (12). As k increases, the curves show a good scaling collapse, in accordance with Eq. (24).

D. Finite- k corrections to Tonks two-particle distribution

In order to compute finite- k corrections to Eq. (23), we evaluate the engine-engine correlation for finite r , k , and δ , with $r \gg 1$, $k \gg 1$, and $\delta \ll 1$, keeping $R = r\delta$, $a = k\delta$, and ρ fixed and finite. Then, on substituting $\rho_0 \approx \frac{\rho}{k(1-\rho)} - \frac{\rho^2}{k^2(1-\rho)^2}$ and $(1-\rho_0) \approx$

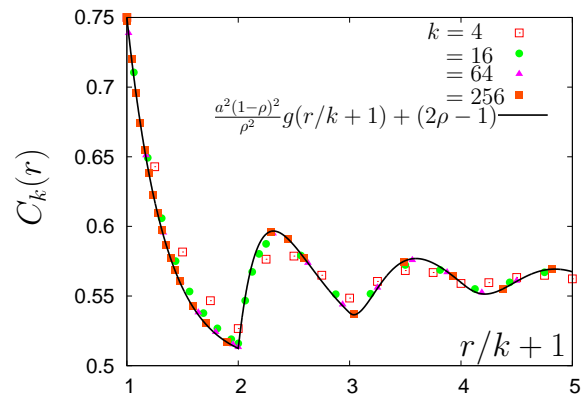


FIG. 5: (Color online) Scaling approach of the density-density correlation $C_k(r)$ to the Tonks limit: $C_k(r)$ vs. $r/k + 1$ at fixed $\rho = 0.75$ and $a = 400$ exhibits data collapse for large k in accordance with Eq. (24). The data are obtained by numerically evaluating Eqs. (9) and (12).

$\exp\left(-\frac{\rho}{k(1-\rho)}\right) \exp\left(\frac{\rho^2}{2k^2(1-\rho)^2}\right)$ into Eq. (9), and keeping terms to leading order in $1/k$, we get

$$k^2 \mathcal{E}_k(r) \approx a^2 g\left(\frac{r}{k}\right) + \frac{\rho}{k} h\left(\frac{r}{k}\right), \quad (25)$$

where

$$h(x) = \sum_{m=1}^{\infty} A(x-m) \frac{(x-m)^{m+1}}{(m-1)!(l-1)^m} \exp\left(-\frac{x-m}{l-1}\right) \times \left[\frac{m(m-1)}{2(x-m)} - \frac{m}{(l-1)} + \frac{x-m}{2(l-1)^2} \right]; \quad x \neq 1. \quad (26)$$

Here, $A(x)$ is the unit step function defined in Eq. (20). Figure 4 shows that inclusion of the leading-order correction to the Tonks result, as in Eq. (25), indeed resolves the discrepancy between $k^2 \mathcal{E}_k(r)$ and $a^2 g(r/k)$.

IV. STEADY STATE DYNAMICS

A. Current and kinematic wave velocity

In discussing the current in the system, we need to distinguish between that associated with the motion of engines, and that with the k -mers. Contributions to the engine current across a bond $(i, i+1)$ arise when either (i) the i -th site is occupied by an engine, while the $(i+1)$ -th site is vacant, or, (ii) the $(i+1)$ -th site is occupied by an engine, while the $(i-k+1)$ -th site is vacant. On using the results of Sec. II C, we find that in the thermodynamic limit, the average engine current in the steady state is given by [11]

$$J_e = \frac{(p-q)\rho(1-\rho)}{\rho + k(1-\rho)}. \quad (27)$$

To compute the k -mer current, J , note that associated with the motion of the engine to an adjacent site is the sliding of the corresponding k -mer across $(k-1)$ bonds, so that $J = kJ_e$. It can be checked that J has a maximum at the density $\rho_c = \sqrt{k}/(\sqrt{k} + 1)$.

The kinematic wave velocity $v_K \equiv \partial J / \partial \rho$ accounts for the transport of density fluctuations through the system in the steady state [25]. We find

$$v_K = k(p - q) \left[\frac{(k-1)\rho^2 + k(1-2\rho)}{[\rho + k(1-\rho)]^2} \right]. \quad (28)$$

Evidently, v_K vanishes if the density is ρ_c . As we discuss below, v_K plays an important role in determining the form of the temporal decay of the density autocorrelation.

B. Mapping to the ASEP: Wheeling velocity

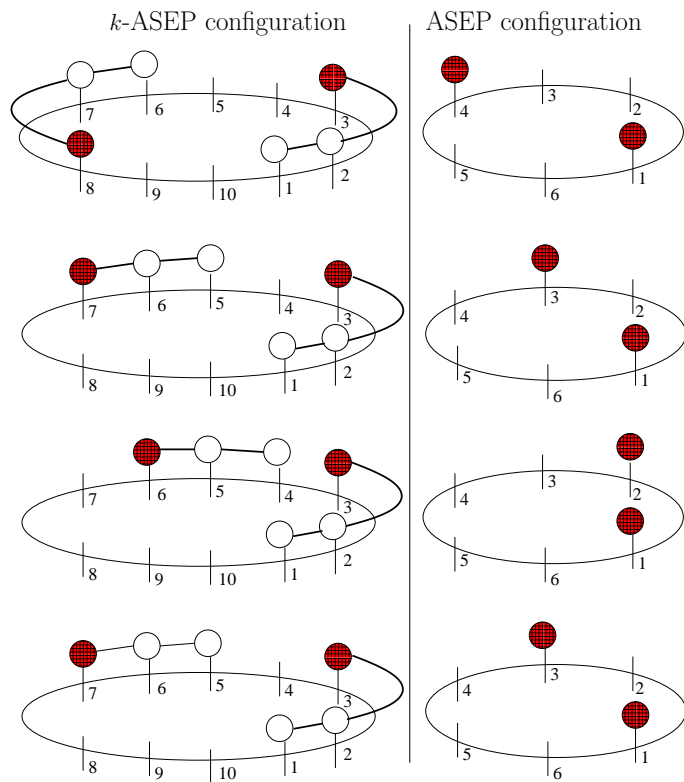


FIG. 6: (Color online) Mapping of a typical k -mer configuration to an ASEP configuration and their subsequent evolution in time. The first site of the ASEP lattice may be defined in more than one way; the figure illustrates one possibility.

We now discuss a mapping of the k -ASEP with a number, N , of k -mers on a 1D periodic lattice of L sites to an ASEP of N hard-core particles on a 1D periodic lattice of $L' = L - N(k-1)$ sites. We show that as a result of the mapping, a fixed site in the k -ASEP corresponds to an

ASEP site that moves around the ASEP ring with a finite mean velocity. This phenomenon is known as wheeling, and the mean velocity is called the wheeling velocity W [17]. This velocity plays an important role in the scaling properties of the temporal density-density correlation of the k -ASEP, as we discuss in the next subsection.

The mapping involves representing each k -mer by a hard-core particle that corresponds to the engine of the k -mer, as illustrated in Fig. 6. In this way, every k -ASEP configuration is mapped to a unique configuration in the ASEP. Associated with the motion of a k -mer is that of the corresponding ASEP particle according to the ASEP dynamics. We now see that the quantity ρ_0 in Eq. (8) is the particle density in the equivalent ASEP.

It can be seen from Fig. 6 that in the process of mapping, the ASEP image of a fixed k -mer site moves around the ASEP lattice as a result of the k -mer motion. For example, consider the transition $(111\dots 1)0 \rightarrow 0(111\dots 1)$. It is easy to see that in this transition, the ASEP images of k -ASEP sites containing the 0 and the leftmost 1 in the string $(111\dots 1)0$ do not change, while the images of those containing the remaining 1's in the string increase by one unit. On the other hand, in the transition $0(111\dots 1) \rightarrow (111\dots 1)0$, the ASEP images of k -ASEP sites containing the 0 and the rightmost 1 in the string $0(111\dots 1)$ do not change, while the images of those containing the remaining 1's in the string decrease by one unit. This motion of an ASEP site corresponding to a fixed site in the k -ASEP is the phenomenon of wheeling. As a result, the displacement of the ASEP image of a fixed k -ASEP site in time t is given by

$$\Delta r(t) = Wt + \phi(t), \quad (29)$$

where $\phi(t)$ is a random variable with zero mean, arising from the stochasticity in the dynamics. Referring to the results on joint occupation probabilities in Sec. II C, we find that the wheeling velocity is given by

$$W = \frac{(p-q)(k-1)\rho(1-\rho)}{\rho + k(1-\rho)}. \quad (30)$$

C. The temporal density-density correlation

The temporal density-density correlation function in the steady state of the k -ASEP is defined as

$$\mathcal{C}_k(r = |i-j|, t) \equiv \langle n_i(0)n_j(t) \rangle - \rho^2, \quad (31)$$

where $n_i(t)$ denotes the occupation index of site i at time t . In particular, the density autocorrelation is given by $\mathcal{C}_k(t) \equiv \mathcal{C}_k(0, t)$.

We study $\mathcal{C}_k(t)$ by performing Monte Carlo simulations of the k -ASEP in the steady state. Figure 7 shows that $\mathcal{C}_k(t)$ oscillates in time. The inset shows that for large k , the autocorrelation for different k at a fixed density ρ is initially a function of t/k . This behavior holds up to a k -dependent time. To understand the dependence of $\mathcal{C}_k(t)$

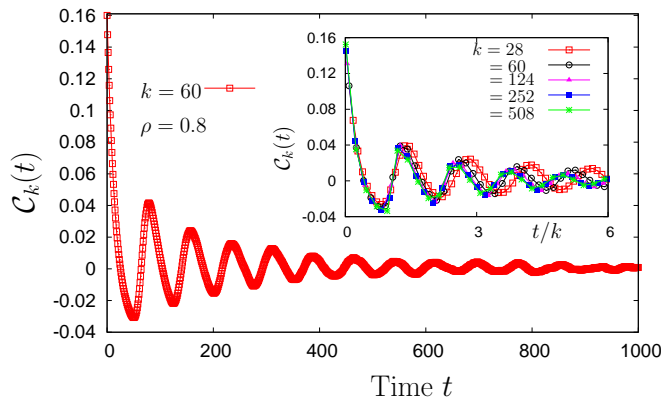


FIG. 7: (Color online) Short-time behavior of the k -ASEP density autocorrelation $C_k(t)$ for $k = 60$ and $\rho = 0.8$. The data are obtained from Monte Carlo simulations. The inset shows $C_k(t)$ vs. t/k at fixed $\rho = 0.8$, illustrating scaling for large k .

on the ratio t/k , we note that at short times, the relevant time scale is set by the time $\tau(k)$ that an occupied site takes to fall vacant. This is consistent with $C_k(t)$ being a function of $t/\tau(k)$. An upper bound on $\tau(k)$ may be estimated as the time $\tau_e(k) \approx k/v_e$, the time that an engine takes to move by its own length. Here v_e is the velocity of an engine, which may be obtained from Eq. (27) as $v_e = \frac{k(p-q)(1-\rho)}{\rho+k(1-\rho)}$. In the limit of large k , one finds that $\tau_e(k) \approx k$, so that $C_k(t)$ is a function of t/k , as observed.

We now discuss the behavior of $C_k(t)$ at long times. To proceed, we examine the function $C_k(r, t)$ for which an earlier study in the case $k = 2$ has illustrated that in the limit of long times and large distances, it assumes a particular scaling form [17]. To obtain the scaling for general k , we utilize the mapping to the ASEP discussed in Sec. IV B and invoke known scaling properties of the density correlation in the latter.

In the ASEP ($k = 1$), the temporal density-density correlation function, $C_1(r = |i-j|, t) \equiv \langle n_i(0)n_j(t) \rangle - \rho_0^2$, in the scaling limit follows the form [26]

$$C_1(r, t) \propto t^{-2/3}F(u); \quad u = \frac{1}{2}(J_0t^2)^{-1/3}(r - v_{0K}t). \quad (32)$$

Here, J_0 and v_{0K} are, respectively, the steady-state current and the kinematic wave velocity in the ASEP, given by $J_0 = (p-q)\rho_0(1-\rho_0)$, and $v_{0K} = (p-q)(1-2\rho_0)$ [2]. In the limit of large u , it is known that $F(u) \sim \exp(-\mu|u|^3)$, with $\mu \simeq -0.295$ [26].

It is evident from the k -ASEP to ASEP mapping discussed above that at long times, neglecting the stochastic part $\phi(t)$ in the displacement of a mapped site in the ASEP, the correlation $C_k(r, t)$ has a behavior similar to $C_1(r + Wt, t)$ [17]. Thus, for a fixed k , in the limit of long

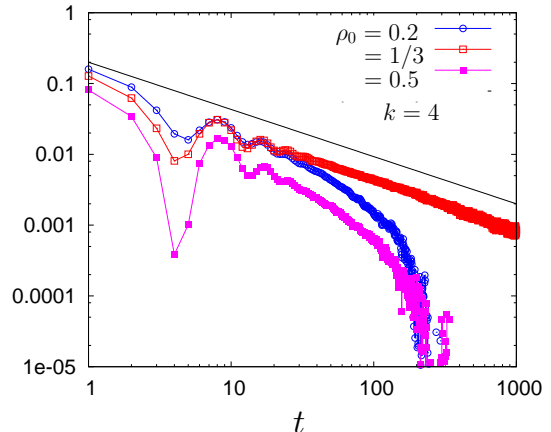


FIG. 8: (Color online) Long-time decay of the k -ASEP density autocorrelation $C_k(t)$, as a power law in time at the compensating density ρ_{0c} , and as an exponential at other densities. The data are obtained from Monte Carlo simulations. Here $k = 4$, so that $\rho_{0c} = 1/3$. The black line has the slope of $-2/3$.

times and large distances, $C_k(r, t)$ follows the scaling form

$$C_k(r, t) \propto t^{-2/3}F(u'); \quad u' = \frac{1}{2}(J_0t^2)^{-1/3}(r + (W - v_{0K})t). \quad (33)$$

The autocorrelation $C_k(t)$ behaves asymptotically as

$$C_k(t) \propto t^{-2/3}e^{-\kappa t}, \quad (34)$$

where κ is a constant determined by the difference $(W - v_{0K})$. Thus, at long times, $C_k(t)$ decays as an exponential in time, unless the density ρ is such that the difference vanishes. In this case, the autocorrelation at late times decays in time as a power law: $C_k(t) \sim t^{-2/3}$. The corresponding ASEP density is called the compensating density ρ_{0c} [17], and satisfies

$$\rho_{0c}^2(k-1) + 2\rho_{0c} - 1 = 0. \quad (35)$$

Solving for the positive root, we get

$$\rho_{0c} = \frac{1}{\sqrt{k+1}}, \quad (36)$$

which matches with the result for $k = 2$ derived in [17]. Note that corresponding to ρ_{0c} is the k -ASEP density of occupied sites ρ_c , mentioned in Sec. IV A, at which the k -mer current J is maximized and the kinematic wave velocity v_K is zero.

Figure 8 shows $C_k(t)$ as a function of time for three values of the ASEP density, namely, the compensating density ρ_{0c} , and two other values on either side. We see an asymptotic $t^{-2/3}$ decay of the autocorrelation at the compensating density and an exponential decay at other densities, in accordance with our analysis above.

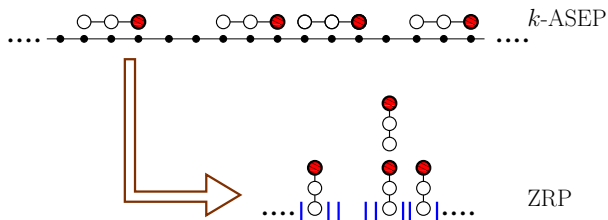


FIG. 9: (Color online) Mapping of the k -ASEP to the ZRP. The k -ASEP vacancies are considered as sites in the ZRP, while an uninterrupted sequence of k -mers in front of a vacancy is regarded as a set of particles occupying the corresponding ZRP site, such that the number of particles equals the number of k -mers in the sequence.

V. ACKNOWLEDGEMENT

Part of this work is based on the Ph. D. thesis of SG at the Tata Institute of Fundamental Research, Mumbai. He acknowledges support of the Israel Science Foundation (ISF), and the French contract ANR-10-CEXC-010-01. We thank G. M. Schütz and R. K. P. Zia for discussions and for pointing out Ref. [20] and Ref. [16], respectively, to us.

Appendix A: Mapping of the k -ASEP to the ZRP

In this appendix, we discuss a mapping of the k -ASEP to a zero-range process (ZRP) and show how static correlations in the former are obtained by using the mapping. This method of obtaining the correlations is an alternative to the one discussed in Sec. III.

In the ZRP, an unrestricted number of particles resides on lattice sites and hops between sites with a rate that depends only on the number of particles on the departure site [18]. Each k -ASEP configuration can be mapped to a unique ZRP configuration in the following way: one considers vacancies (0's) in the k -ASEP as sites in the ZRP and an uninterrupted sequence of k -mers following a vacancy as particles residing on the corresponding ZRP site, with the number of particles equal to the number of k -mers in the sequence. The ZRP has N particles and $M \equiv L - Nk$ sites labeled by the index i . A generic ZRP configuration is the set $\{m_i\} \equiv (m_1, m_2 \dots m_M)$, where m_i is the number of particles on the i -th site (see Fig. 9). The motion of a k -mer in the k -ASEP translates to hopping of a particle from a ZRP site to its right or left neighbor with rates p or q , respectively.

For an arbitrary hop rate, the ZRP has a product measure stationary state [18]. In our case, where the rates do not depend on the number of particles on the departure site, the steady-state weight of any configuration $\{m_i\}$ is

$$P(\{m_i\}) = \prod_i f(m_i) \delta\left(N - \sum_{i=1}^M m_i\right), \quad f(m) = 1. \quad (\text{A1})$$

The delta function stands for overall particle conservation.

The steady state weight of any k -ASEP configuration is obtained by mapping it to a configuration in the equivalent ZRP and computing its weight by utilizing Eq. (A1). In our case, since $f(m) = 1$ for all m , all k -ASEP configurations with a given number, N , of k -mers are equally likely. Now, using the formalism discussed in [19], one may rewrite the steady-state weight of any k -ASEP configuration (n_1, n_2, \dots, n_L) in a matrix product form by replacing each occupation number n_i by either a matrix D or a matrix E depending on whether n_i is 1 or 0, respectively. From the correspondence between the k -ASEP and the ZRP, we have

$$P(\{m_i\}) = \text{Tr}[ED^{km_1} \dots ED^{km_M}] \delta\left(N - \sum_{i=1}^M m_i\right), \quad (\text{A2})$$

where Tr denotes the usual matrix trace operation.

Without loss of generality, one may take $E = |\alpha\rangle\langle\beta|$, where the vectors $|\alpha\rangle$ and $\langle\beta|$ are to be determined. This choice of E together with Eqs. (A2) and (A1) demand that for any positive integer m , the matrix D satisfies

$$\langle\beta|D^{mk}|\alpha\rangle = f(m) = 1. \quad (\text{A3})$$

Also, $\langle\beta|D^j|\alpha\rangle = 0$ for positive integers j which are not multiples of k . A simple k -dimensional representation of matrices E and D is when they have non-zero elements $E_{11} = 1$ and $D_{k1} = 1 = D_{i,i+1}$, that is,

$$E = |\alpha\rangle\langle\beta|, \quad \text{with} \quad |\alpha\rangle = |1\rangle, \quad \langle\beta| = \langle 1|, \\ D = \sum_{i=1}^{k-1} |i\rangle\langle i+1| + |k\rangle\langle 1|. \quad (\text{A4})$$

Here, the set $\{|i\rangle\}$ represents the standard basis vectors in k -dimensions. This choice ensures that the weight of any configuration with one or more blocks of l particles is zero if l is not an integral multiple of k ; all other configurations are equally probable.

Let us mention that the matrix formulation discussed above is different from the Matrix Product Ansatz (MPA) of Derrida *et al.* [27], in which matrices satisfy specific algebraic relations dictated by the system dynamics. For models with ZRP correspondence, the matrices generically satisfy Eq. (A3), and therefore, depend only on the weights $f(m)$. It is always possible to get one representation of these matrices, whereas finding explicit representation of the MPA matrices is non-trivial.

Partition function $Z_L(z)$: The first task in computing k -ASEP static correlations is to find the partition function of the system, which is conveniently done in the grand canonical ensemble by associating the fugacity z with any occurrence of the matrix D . This gives $Z_L(z) = \text{Tr}[C^L]$, where $C = zD + E$. The configuration with no vacant site is not dynamically accessible. Thus, $Z_L(z)$ is given by weights of all configurations with at

least one vacant site:

$$\begin{aligned} Z_L(z) &= \sum_{n=1}^L \text{Tr} [(zD)^{n-1} EC^{L-n}] \\ &= \sum_{n=1}^L \langle \beta | C^{L-n} (zD)^{n-1} | \alpha \rangle. \end{aligned} \quad (\text{A5})$$

To proceed, we use the following generating function:

$$\begin{aligned} \mathcal{Z}(z, \gamma) &= \sum_{L=1}^{\infty} \gamma^L Z_L(z) = \langle \beta | \frac{\gamma}{\mathcal{I} - \gamma C} \frac{1}{\mathcal{I} - \gamma z D} | \alpha \rangle \\ &= \frac{\gamma [1 + (k-1)(\gamma z)^k]}{[1 - \gamma - (\gamma z)^k][1 - (\gamma z)^k]}, \end{aligned} \quad (\text{A6})$$

where \mathcal{I} is the k -dimensional identity matrix. Note that $\mathcal{Z}(z, \gamma)$ may be interpreted as the partition function in the variable length ensemble. The parameters z and γ together determine macroscopic observables like the density of occupied sites and the average system size. The density of occupied sites is $\rho = 1 - \langle \bar{n}_i \rangle$, where

$$\langle \bar{n}_i \rangle = \frac{\gamma}{\mathcal{Z}} \langle \beta | \frac{1}{\mathcal{I} - \gamma C} | \alpha \rangle = \frac{1 - (\gamma z)^k}{1 + (k-1)(\gamma z)^k}. \quad (\text{A7})$$

The average system size is given by $\langle L \rangle = \frac{\gamma}{\mathcal{Z}} \frac{\partial \mathcal{Z}}{\partial \gamma}$.

One may check that $\langle L \rangle$ has the radius of convergence

$$z^* = \frac{1}{\gamma} (1 - \gamma)^{1/k}. \quad (\text{A8})$$

Thus, the thermodynamic limit $\langle L \rangle \rightarrow \infty$ is achieved at $z = z^*$, when every observable of the system becomes a function of γ *only*. For example, ρ is obtained from Eq. (A7) as $\rho = \frac{k(1-\gamma)}{\gamma+k(1-\gamma)}$, which may be inverted to obtain

$$\gamma = \frac{k(1-\rho)}{\rho+k(1-\rho)} = 1 - \rho_0. \quad (\text{A9})$$

Equal-time correlations $V_k(r), \mathcal{E}_k(r)$: One may compute $V_k(r)$ by writing it in terms of matrices as follows:

$$\begin{aligned} V_k(r) &= \frac{\gamma^{r+1}}{\mathcal{Z}} \langle \beta | C^{r-1} | \alpha \rangle \langle \beta | \frac{1}{\mathcal{I} - \gamma C} | \alpha \rangle \\ &= \gamma^r (1 - \rho) \langle \beta | C^{r-1} | \alpha \rangle. \end{aligned} \quad (\text{A10})$$

Now, for any integer j , one may check that

$$\langle \beta | C^j | \alpha \rangle = \sum_{m=0}^{\lfloor j/k \rfloor} \binom{j - mk + m}{m} z^{mk}, \quad (\text{A11})$$

which results in

$$V_k(r) = \gamma^r (1 - \rho) \sum_{m=0}^{\lfloor (r-1)/k \rfloor} \Omega_{m, r-1}^{\text{free}} z^{mk}.$$

The equal-time engine-engine correlation $\mathcal{E}_k(r)$ may be similarly calculated by using the matrix formulation:

$$\begin{aligned} \mathcal{E}_k(r) &= \frac{\gamma^{r+k}}{\mathcal{Z}} \langle \beta | \frac{1}{\mathcal{I} - \gamma C} | \alpha \rangle \sum_{m=0}^{\lfloor (r-k)/k \rfloor} \Omega_{m, r-k}^{\text{free}} z^{(m+2)k} \\ &= (1 - \rho) \gamma^{r+k-1} \sum_{m=0}^{\lfloor (r-k)/k \rfloor} \Omega_{m, r-k}^{\text{free}} z^{(m+2)k}. \end{aligned} \quad (\text{A12})$$

In the thermodynamic limit, using Eq. (A8), we get

$$\begin{aligned} V_k(r) &= \frac{\gamma^{r+1}}{\gamma + k(1-\gamma)} \sum_{m=0}^{\lfloor (r-1)/k \rfloor} \Omega_{m, r-1}^{\text{free}} \left(\frac{1-\gamma}{\gamma^k} \right)^m, \\ \mathcal{E}_k(r) &= \frac{\gamma^{r+k}(1-\gamma)^2}{\gamma + k(1-\gamma)} \sum_{m=0}^{\lfloor (r-k)/k \rfloor} \Omega_{m, r-k}^{\text{free}} \left(\frac{1-\gamma}{\gamma^k} \right)^m. \end{aligned}$$

Replacing γ by $1 - \rho_0$ in the expressions on the right reduce them to those in Eqs. (16) and (9), respectively.

-
- [1] T. M. Liggett, *Interacting Particle Systems* (Springer-Verlag, New York, 1985).
- [2] G. M. Schütz, in *Phase Transitions and Critical Phenomena*, edited by C. Domb and J. L. Lebowitz (Academic Press, San Diego, 2001), Vol. 19.
- [3] O. Golinelli and K. Mallick, *J. Phys. A: Math. Gen.* **39**, 12679 (2006).
- [4] R. K. P. Zia, J. J. Dong and B. Schmittmann, *J. Stat. Phys.* **144**, 405 (2011).
- [5] T. Chou, K. Mallick, and R. K. P. Zia (unpublished).
- [6] C. T. MacDonald, J. H. Gibbs, and A. C. Pipkin, *Biopolymers* **6**, 1 (1968).
- [7] C. T. MacDonald and J. H. Gibbs, *Biopolymers* **7**, 707 (1969).
- [8] T. Sasamoto and M. Wadati, *J. Phys. A: Math. Gen.* **31**, 6057 (1998).
- [9] F. C. Alcaraz and R. Z. Bariev, *Phys. Rev. E* **60**, 79 (1999).
- [10] G. Lakatos and T. Chou, *J. Phys. A: Math. Gen.* **36**, 2027 (2003).
- [11] L. B. Shaw, R. K. P. Zia and K. H. Lee, *Phys. Rev. E* **68**, 021910 (2003).
- [12] L. B. Shaw, A. B. Kolomeisky and K. H. Lee, *J. Phys. A: Math. Gen.* **37**, 2105 (2004).
- [13] L. B. Shaw, J. P. Sethna and K. H. Lee, *Phys. Rev. E* **70**, 021901 (2004).
- [14] G. Schönherr and G. M. Schütz, *J. Phys. A: Math. Gen.* **37**, 8215 (2004).
- [15] J. J. Dong, B. Schmittmann, and R. K. P. Zia, *Phys. Rev. E* **76**, 051113 (2007).
- [16] J. J. Dong, Ph. D. Thesis, Virginia Polytechnic Institute and State University, 2008. Thesis available at <http://scholar.lib.vt.edu/theses/available/etd-04092008-113617/>
- [17] M. Barma, M. D. Grynberg, and R. B. Stinchcombe, *J. Phys.: Condens. Matter* **19**, 065112 (2007).
- [18] M. R. Evans and T. Hanney, *J. Phys. A: Math. Gen.* **38**,

- R195 (2005).
- [19] U. Basu and P. K. Mohanty, *J. Stat. Mech.: Theory Exp.* L03006 (2010).
- [20] G. Schönherr, *Phys. Rev. E* **71**, 026122 (2005).
- [21] L. Tonks, *Phys. Rev.* **50**, 955 (1936).
- [22] Z. W. Salsburg, R. W. Zwanzig, and J. G. Kirkwood, *J. Chem. Phys.* **21**, 1098 (1953).
- [23] G. I. Menon, M. Barma, and D. Dhar, *J. Stat. Phys.* **86**, 1237 (1997).
- [24] J-L Barrat and J-P Hansen, *Basic Concepts for Simple and Complex Liquids* (Cambridge University Press, Cambridge, 2003).
- [25] M. J. Lighthill and G. B. Whitham, *Proc. R. Soc. London A* **229**, 281 (1955).
- [26] M. Prähofer and H. Spohn, in *In and Out of Equilibrium (Progress in Probability Vol. 51)*, edited by V. Sidoravicius (Boston, MA: Birkhauser, 2002), pp 185-204; also, eprint:arXiv:cond-mat/010200.
- [27] B. Derrida, M. R. Evans, V. Hakim, and V. Pasquier, *J. Phys. A: Math. Gen.* **26**, 1493 (1993); R. A. Blythe and M. R. Evans, *J. Phys. A: Math. Theor.* **40**, R333 (2007).